



HAL
open science

An ab-initio evaluation of the local effective interactions in the Na_xCoO₂ family

Sylvain Landron, Soret Julien, Marie-Bernadette Lepetit

► **To cite this version:**

Sylvain Landron, Soret Julien, Marie-Bernadette Lepetit. An ab-initio evaluation of the local effective interactions in the Na_xCoO₂ family. 2008. hal-00281033v1

HAL Id: hal-00281033

<https://hal.science/hal-00281033v1>

Preprint submitted on 20 May 2008 (v1), last revised 7 Jul 2010 (v2)

HAL is a multi-disciplinary open access archive for the deposit and dissemination of scientific research documents, whether they are published or not. The documents may come from teaching and research institutions in France or abroad, or from public or private research centers.

L'archive ouverte pluridisciplinaire **HAL**, est destinée au dépôt et à la diffusion de documents scientifiques de niveau recherche, publiés ou non, émanant des établissements d'enseignement et de recherche français ou étrangers, des laboratoires publics ou privés.

An ab-initio evaluation of the local effective interactions in the $\text{Na}_{0.5}\text{CoO}_2$

Sylvain Landron¹ and Marie-Bernadette Lepetit¹

¹CRISMAT, ENSICAEN-CNRS UMR6508, 6 bd. Maréchal Juin, 14050 Caen, FRANCE

(Dated: May 20, 2008)

We used quantum chemical ab initio methods to determine the effective parameters of Hubbard and $t-J$ models for the $\text{Na}_{0.5}\text{CoO}_2$ compound. As for the superconducting compound we found the a_{1g} cobalt orbitals 260 meV (Co(1)) and 320 meV (Co(2)) above the e'_g ones. These orbital order is explained by the e'_g-e_g hybridization of the cobalt $3d$ orbitals. The effective exchange integrals are found strongly reduced compared to the superconducting system with values ranging from -11 to -27 meV according to the bonds. In fact, surprisingly, the magnetic exchanges in the CoO_2 layers, are found strongly dependant of the weak local structural distortions.

I. INTRODUCTION

Since the discovery of the large thermoelectric power¹ and then of superconductivity² in the Na_xCoO_2 layered cobaltate family, these systems have attracted a lot of attention. Indeed, they present a very rich phases diagram as a function of the sodium content x and the possible water intercalation. For small x ($0 < x < 0.5$) the system is a paramagnetic metal, while for larger x ($0.5 < x < 0.75$) it is a Curie-Weiss metal. Over 0.75, the system can be seen as a weakly ferromagnetic metal³, however neutron diffraction measurements⁴ rather sees A-type antiferromagnetism, that is ferromagnetic CoO_2 layers, antiferromagnetically coupled. For special values of the sodium content, $x = 1/4$, $x = 1/2$ ⁵ and $x = 1$, the system is insulating. A band insulator for $x = 1$ and a charge/spin ordered state for $x = 0.5$.

The Na_xCoO_2 compounds are composed of CoO_2 layers in the (\vec{a}, \vec{b}) plane, between which the sodium ions are located. The CoO_2 layers are formed by CoO_6 edge-sharing octahedra forming a two-dimensional triangular lattice of cobalt ions. The CoO_6 octahedra present a trigonal distortion along the crystallographic \vec{c} axis corresponding to a compression of the oxygen planes toward the cobalt one. Additional distortions take place, according to the sodium ordering. In the $\text{Na}_{0.5}\text{CoO}_2$ compound (P2 structure), subject of the present work, the sodiums ordering is commensurate and presents two types of alternated stripes along the \vec{b} direction⁶. In the first stripes, the sodium atoms are located on-top of (below) the cobalts atoms, and in the second type of stripes the sodium ions are located on-top of (below) the center of the cobalt triangles (see figure 1). It results two types of cobalt atoms organized in stripes along the \vec{b} direction, namely the Co(1) atoms (located on top of a sodium ion) and the Co(2) ones. Compared to the superconducting compound $\text{Na}_{0.3}\text{CoO}_2 - 1.3\text{H}_2\text{O}$, the present system exhibit a enlarged CoO_2 layer. Indeed, the average Co-O distances are 1.887Å for Co(1) and 1.900Å for Co(2) to be compared to the 1.855Å in the superconductor. Similarly, the average trigonal distortions of the CoO_6 octahedra are weaker, with 58.9 degree between the \vec{c} axis and the Co(1)-O directions, and 59.4 degrees (Co(2)), to be compared to 61.5 degrees for $\text{Na}_{0.3}\text{CoO}_2 - 1.3\text{H}_2\text{O}$.

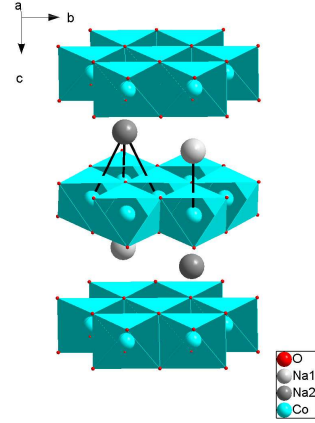


FIG. 1: Schematic structure of the $\text{Na}_{0.5}\text{CoO}_2$ compound. The black lines connect the Na^+ ions with their nearest cobalt neighbors.

One can thus expect a lowering of the cobalt $3d$ orbital splitting due to the crystalline field.

Out of all the Na_xCoO_2 systems, the $x = 0.5$ compound presents a very rich but not well understood phase diagram. Indeed, the Na^+ ions order at very large temperature, namely slightly above 300 K⁷, inducing a small charge order in the cobalt layer. Despite this small charge order the system remains conducting. At 88 K a magnetic phase transition occurs, associated with a structural distortion, and the onset of a long range magnetic order. Again, despite this transition, the system remains conducting up to 53 K where a small charge gap (14 meV) finally opens^{5,8}.

The understanding of this complex phase diagram is still under process. Different hypotheses have been advanced such as successive Fermi surface nesting⁹, polarons formation¹⁰, one band versus three bands crossover¹¹.

In order to understand the low energy physics of this compound it is thus necessary to have accurate determination of the pertinent degrees of freedom and of their coupling, as a function of the exact crystallographic structure. Indeed, all authors agree on the importance of the sodium ordering and the induced cobalt local envi-

ronment distortions, on the low energy properties. The aim of this paper is to provide such informations using state of the art quantum chemical spectroscopy methods. The next section will shortly recall the methods. Section III will presents our results and finally the last section will sum up our conclusions.

II. METHOD AND COMPUTATIONAL DETAILS

The method used in this work (CAS+DDCI¹²) is a configurations interaction method, that is an exact diagonalization method within a selected set of Slater determinants, on embedded crystal fragments. This method has been specifically designed to accurately treat strongly correlated systems, for which there is no single-determinant description. The main point is to treat exactly all correlation effects and exchange effects within a selected set of orbitals (here the $3d$ shell of the cobalt atoms) as well as the excitations responsible for the screening effects on the exchange, repulsion, hopping, etc. integrals.

The CAS+DDCI method has proved very efficient to compute, within experimental accuracy, the local interactions (orbital energies, atomic excitations, exchange and transfer integrals, coulomb repulsion etc.) of a large family of strongly correlated systems such as high T_c copper oxides¹³, vanadium oxides¹⁴, nickel and cuprate fluorides¹⁵, spin chains and ladders¹⁶, etc.

The clusters used in this work involve one and two cobalt atoms (CoO_6 and Co_2O_{10}) and their oxygen first coordination shell (see figure 2). These fragments are embedded in a bath designed so that to reproduce on them the main effects of the rest of the crystal ; that is the Madelung potential and the exclusion effects of the electrons of the other atoms of the crystal on the clusters electrons.

The electrostatic potential is reproduced by a set of point charges located at the atomic positions. The charges are renormalized next to the bath borders in order to obtain an exponential convergence of the Madelung potential¹⁷. The convergence accuracy was set in the present work to the milli-electron-Volt. The nominal atomic charges used in this work are the formal charges, that is $+3.5$ for the cobalt atoms, -2 for the oxygen atoms and $+1$ for the sodium atoms. The exclusion effects are treated using total ions pseudo-potentials¹⁸ (TIP) on the first shell of atomic sites surrounding the clusters.

The calculations were done using the MOLCAS¹⁹ and CASDI²⁰ suite of programs. The basis sets used can be found in reference²¹. The structural parameter were taken from the 10 K data of reference 6.

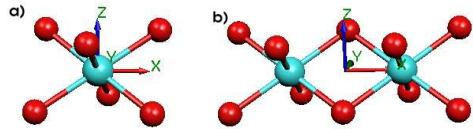


FIG. 2: a) CoO_6 and b) Co_2O_{10} clusters used in the present calculations.

III. RESULTS

A. On site orbital energy splitting and charge order

A strong controversy has been going on in the literature about the cobalt $3d$ orbital splitting. Indeed, authors did not agree on the relative order of the t_{2g} orbitals under the trigonal distortion of the regular octahedron ($T_{2g} \rightarrow A_{1g} \oplus E_g$). The origin of the controversy was the fact that the crystalline field theory²² as well as some LDA calculations²³ found the a_{1g} orbital of lower energy than the e'_g ones, while other density functional calculations²⁴, as well as quantum chemical calculations²⁵ or ARPES experimental results²⁶ found them of reverse order. We recently showed²⁷ that the origin of the controversy was an incorrect treatment of the exchange and correlation integrals within the $3d$ shell. Indeed, only when these effects are taken into account with their whole complexity, the relative order between the a_{1g} and e'_g orbitals issued from the t_{2g} is correctly predicted. This splitting is one of the crucial parameter for the determination of the nature of Fermi level states as recently shown by Marianetti *et al*²⁸.

We thus computed the t_{2g} orbitals splitting in the $\text{Na}_{0.5}\text{CoO}_2$ compound, for the two different cobalt sites. These values can be extracted from the spectroscopy of the CoO_6 embedded fragments. Indeed, the excitation energy between the three cobalt states, where one hole is located one of the t_{2g} orbitals, yield the effective splittings between the a_{1g} and e'_g orbitals. The relative order of the t_{2g} orbitals is displayed on figure 3. One sees im-

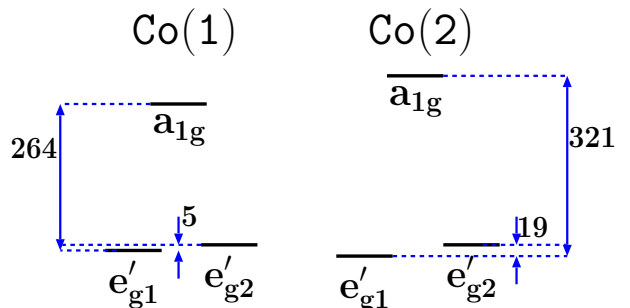


FIG. 3: Schematic representation of the effective cobalt t_{2g} orbital energies in meV. Let us recall that the Co(1) cobalt is located directly under or on top a Na^+ ion.

mediately that the a_{1g} orbitals are on both sites about 250–300 meV higher than the e'_g ones. Similarly, in our dimer calculations we see that the $\text{Co}^{4+}(1)$ ion is globally of lower energy than the $\text{Co}^{4+}(2)$ ion. Indeed, our calculations yield a global charge order of about 0.17 electrons in favor of the Co(1) site. This result is in agreement with the common sense expectations that will favor a smaller valence for the cobalt with the largest number of Na^+ cations neighbors. Indeed, computing the electrostatic potential difference between the two cobalt sites one finds the Co(1) site about 315 meV lower than the Co(2) site. This result is however in contradiction with the Bond Valence Sum (BVS) model, since the later yields a charge ordering of 0.12 electron in favor of the Co(2) site⁶, however it is in agreement with the LDA+U calculations²⁹ ($\sim 0.16\bar{e}$ in favor of Co(1)).

B. Orbital hybridization

Let us now focus on the cobalt 3d orbital hybridization. These orbitals can hybridize in two ways : with the oxygen ligands 2p orbitals, but also within the cobalt 3d shell between the t_{2g} and e_g sets of the regular octahedron. Indeed, it was shown (see ref. 27 for details) that not only this hybridization is symmetry allowed by the trigonal distortion of the octahedron, but also that it is responsible for the lowering of the e'_g orbitals compared to the a_{1g} one. The t_{2g} – e_g hybridization angle is reported in table I and found to be a little weaker in this system than in the superconducting compound, as expected from the lower trigonal distortion of the CoO_2 layer in this system. Indeed, the hybridization angle is about 13 degrees in the latter²⁷. Let us now focus on the cobalt ligand

Atom	e'_{g1}	e'_{g2}
Co(1)	-11.59	-8.21
Co(2)	-11.54	-10.18

TABLE I: t_{2g} – e_g mixing angle (degrees) in the occupied e'_g cobalt orbitals.

hybridization. This hybridization seems quite insensitive to the local environment of the cobalt since we find similar values for both crystallographic sites. For the e'_g and a_{1g} orbitals the hybridization accounts for $\sim 10\%$. For the e_g orbitals the hybridization depends on the cobalt average charge with $\sim 45\%$ for a formal Co^{4+} ion and $\sim 30\%$ for a formal cobalt charge of 3.5.

C. Interatomic interactions

Let us now focus on the interactions between two first neighbor cobalt atoms. Many authors assume that the low energy physics of this compound is determined by the a_{1g} orbitals only. We thus computed the effective integrals both for a t – J model and a one-band Hubbard model.

Analyzing the low temperature crystallographic structure of $\text{Na}_{0.5}\text{CoO}_2$ (10 K data of reference 6), one sees that there are four types of independant Co–Co bonds (see figure 4), the Co(1)–Co(1) bond, the Co(2)–Co(2) bond and two kinds of Co(1)–Co(2) bonds, namely those where the cobalt–cobalt interactions are mediated by one O(1) and one O(3) oxygen ligands and those where the cobalt–cobalt interactions are mediated by one O(2) and one O(3) oxygen ligands. The effective magnetic ex-

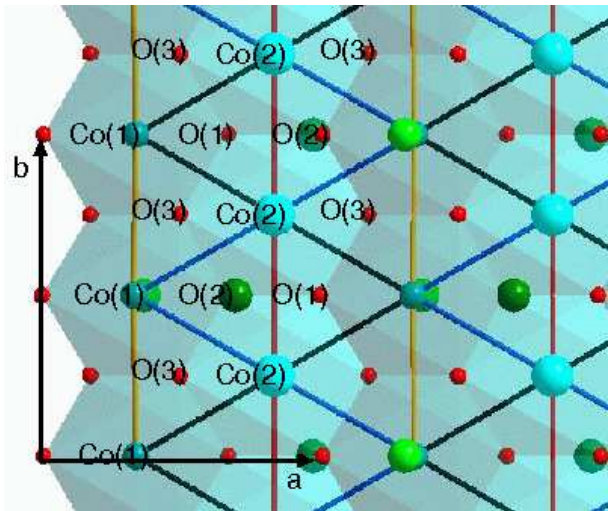


FIG. 4: (color online) Schematic representation of the CoO_2 layers in the $\text{Na}_{0.5}\text{CoO}_2$ compound. There are two different cobalt sites represented in light and darker turquoise color blue, three different oxygen ligands and the four different Co–Co bonds represented in orange [Co(1)–Co(1)], red [Co(2)–Co(2)], dark blue [Co(1)–Co(2) bridged by O(2) and O(3) oxygens] and black [Co(1)–Co(2) bridged by O(1) and O(3) oxygens].

change integrals are

$$\begin{aligned} J(11) &= -11 \text{ meV} & J(22) &= -27 \text{ meV} \\ J(12^{[13]}) &= -19 \text{ meV} & J(12^{[23]}) &= -19 \text{ meV} \end{aligned}$$

where $J(ij)$ refers to the Co(i)–Co(j) bond and the $[ab]$ superscript refers to the bridging oxygens. In our notations, the negative integrals correspond to antiferromagnetic coupling. We find all exchange integrals in the $\text{Na}_{0.5}\text{CoO}_2$ compound antiferromagnetic in agreement with the neutron scattering data³⁰. One notice that the exchange integrals are strongly modulated according to the local environment. Indeed, they differ by a factor larger than two. It results a strongly anisotropic t – J model.

Let us now focus on the hopping integrals. One can get them either from the charge fluctuation in the singlet state of the Co^{4+} – Co^{4+} fragments, or from the spectroscopy of the Co^{3+} – Co^{4+} fragments. A simple analysis shows that the two hopping integrals are somewhat different. In the first case, there is only one spectator electron on the bond, while in the second case, there are



FIG. 5: Schematic representation of the effective hopping integrals as a function of the spectator electrons on the bond. l and r labels refers to the arbitrary “left” and “right” atoms in the fragment.

two of them (see figure 5). It results in a different evaluation of the hopping integrals according to the number of spectator electrons.

$$t(1\bar{e}) = \langle d_l | h | d_r \rangle + \langle d_l \bar{d}_l | 1/r_{12} | d_r \bar{d}_l \rangle$$

$$t(2\bar{e}) = \langle d_l | h | d_r \rangle + \langle d_l \bar{d}_l | 1/r_{12} | d_r \bar{d}_l \rangle + \langle d_l \bar{d}_r | 1/r_{12} | d_r \bar{d}_r \rangle$$

where the l and r labels refers to the arbitrary “left” and “right” atoms in the fragment, and h is the single electron Hamiltonian part.

$t(1\bar{e})$ can be extracted from the $\text{Co}^{4+}-\text{Co}^{4+}$ fragment. Indeed, mapping a single band Hubbard model on the computed low-energy singlet and triplet states wave functions and energies, one gets after a little algebra

$$t(1\bar{e}) = J \frac{1}{2 \cos \varphi \tan \alpha} \quad (1)$$

$$\bar{U} - V = J \left(1 - \frac{1}{\cos 2\varphi \tan^2 \alpha} \right) \quad (2)$$

assuming the following form for the computed singlet and triplet wave functions

$$\psi_{Sg} = \cos \alpha \frac{|d_l \bar{d}_r\rangle + |d_r \bar{d}_l\rangle}{\sqrt{2}}$$

$$+ \sin \alpha \left(\cos \varphi \frac{|d_l \bar{d}_l\rangle + |d_r \bar{d}_r\rangle}{\sqrt{2}} + \sin \varphi \frac{|d_l \bar{d}_l\rangle - |d_r \bar{d}_r\rangle}{\sqrt{2}} \right)$$

$$+ \text{small terms}$$

$$\psi_{Tp} = \frac{|d_l \bar{d}_r\rangle - |d_r \bar{d}_l\rangle}{\sqrt{2}} + \text{small terms}$$

$J = E_{Sg} - E_{Tp}$. $\bar{U} - V$ is the effective on-site repulsion of a simple Hubbard model. Let us remind that it accounts for both the average on-site repulsion between the two sites, $\bar{U} = (U_l + U_r)/2$, and the nearest neighbor effective repulsion between the cobalt atoms, $V = V_{lr}$. The (electron-)hopping integrals between the a_{1g} orbitals thus come as

$$t_{00}^{1\bar{e}}(11) = 84 \text{ meV} \quad t_{00}^{1\bar{e}}(22) = 139 \text{ meV}$$

$$t_{00}^{1\bar{e}}(12^{[13]}) = 115 \text{ meV} \quad t_{00}^{1\bar{e}}(12^{[23]}) = 111 \text{ meV}$$

Once again, one sees that the effective transfer integrals are strongly dependant on the local environment of the cobalts and that the $\text{Na}_{0.5}\text{CoO}_2$ system is more anisotropic than first thought.

The transfer integrals with two spectator electrons on the bond, $t^{2\bar{e}}$, can be extracted from the low-energy states

of the $\text{Co}^{3+}-\text{Co}^{4+}$ fragments. There are six low energy states according to the localization of the hole on the a_{1g} and e'_g orbitals. The associated effective Hamiltonian can be written as

$$H = \begin{pmatrix} a_{1g}^l & e'_{g1}{}^l & e'_{g2}{}^l & a_{1g}^r & e'_{g1}{}^r & e'_{g2}{}^r \\ \varepsilon_0^l & tp_{10}^l & tp_{20}^l & t_{00}^{2\bar{e}} & t_{10}^{2\bar{e}} & t_{20}^{2\bar{e}} \\ tp_{10}^l & \varepsilon_1^l & tp_{12}^l & t_{10}^{2\bar{e}} & t_{11}^{2\bar{e}} & t_{12}^{2\bar{e}} \\ tp_{20}^l & tp_{12}^l & \varepsilon_2^l & t_{20}^{2\bar{e}} & t_{12}^{2\bar{e}} & t_{22}^{2\bar{e}} \\ t_{00}^{2\bar{e}} & t_{10}^{2\bar{e}} & t_{20}^{2\bar{e}} & \varepsilon_0^r & tp_{10}^r & tp_{20}^r \\ t_{10}^{2\bar{e}} & t_{11}^{2\bar{e}} & t_{12}^{2\bar{e}} & tp_{10}^r & \varepsilon_1^r & tp_{12}^r \\ t_{20}^{2\bar{e}} & t_{12}^{2\bar{e}} & t_{22}^{2\bar{e}} & tp_{20}^r & tp_{12}^r & \varepsilon_2^r \end{pmatrix} \quad (3)$$

where ε_i are the atomic effective orbital energies (see figure 3), $t_{ij}^{2\bar{e}}$ are the effective transfer integrals (direct plus mediated by the oxygen ligands) between the $3d_i$ orbital of one cobalt and $3d_j$ of the other. tp_{ij} are effective intra-atomic transfer integrals between the d_i and d_j orbitals of the same atom. One may be surprised to find such terms, since the direct integrals are zero by Y_l^m symmetry, however the coupling with the bridging oxygen $2p$ orbitals yield in second order perturbation theory an effective intra-atomic transfer term of

$$tp_{ij} = - \sum_p \frac{t_{ip} t_{jp}}{\Delta_p}$$

where i and j refers to the $3d$ orbitals of the same cobalt atom, the sum over p runs over all the ligand bridging orbitals, t_{ip} is the cobalt $3d_i$ -ligand hopping integrals and Δ_p is the excitation energy toward the ligand-to-metal charge transfer configuration. For a more detailed description of the underlying mechanism, one can refer to reference 25. Summing the tp_{ij} contributions coming from the six oxygens around a cobalt atom, one can show that they exactly cancel out in a symmetric system. In the present system, where the atomic S_6 symmetry is not exactly respected, these terms will certainly not exactly cancel out, however, one can expect that their sum will remain very weak.

Table II displays the different effective integrals involved in matrix 3. One sees immediately that the dom-

Bond	Inter-atomic transfers (meV)					
	$t_{00}^{2\bar{e}}$	$t_{11}^{2\bar{e}}$	$t_{22}^{2\bar{e}}$	$t_{10}^{2\bar{e}}$	$t_{20}^{2\bar{e}}$	$t_{12}^{2\bar{e}}$
Co(1)-Co(1)	225	-261	-4	-22	-18	-27
Co(2)-Co(2)	281	-325	-11	± 10	-18	± 10

TABLE II: Effective (electron-)hopping integrals between a_{1g} and e'_g orbitals of two neighboring cobalt atoms (in meV).

inant transfer integrals are the inter-atomic hopping between two a_{1g} orbitals and two e'_{g1} orbitals, in agreement with what we found on the superconducting compound. All other integrals are relatively weak (< 30 meV) and can probably be omitted in a simple model. Comparing these values with what we found on the superconductor

system, one sees that they are of the same order of magnitude, except for the inter-atomic hopping between the a_{1g} orbital of one cobalt and the e'_{g2} orbital of the other. Indeed, the larger value found in the superconducting systems (-53 meV) is now spread over the three $t_{10}^{2\bar{e}}$, $t_{20}^{2\bar{e}}$ and $t_{12}^{2\bar{e}}$ hopping terms, due to local symmetry breaking.

Let us notice that as in the hydrated system, the above hopping integrals are of the same order of magnitude as the atomic orbital energy splitting and thus it remains quite difficult to conclude on the pertinence of the one or three bands models. In any case, it does not seem to us that the present results differ enough from those found for the hydrated compound to support the hypothesis of a change in behavior (one-band versus three-bands¹¹) at $x = 0.5$. Let us notice that this hypothesis comes from LDA+U calculations and is strongly dependent of the on-site repulsion U parameter.

D. On-site repulsion

Let us now examine what we find for on-site the repulsion U from our calculations. Indeed, as detailed in equation 2, the value of $\bar{U} - V$ can be extracted from the singlet and triplet energies and wave functions on the $\text{Co}^{4+} - \text{Co}^{4+}$ fragments. It comes for the two cobalt sites and for a single band model

$$\begin{aligned} U(1) - V(11) &= 2.614 \text{ eV} \\ U(2) - V(22) &= 2.859 \text{ eV} \\ \bar{U} - V(12^{[13]}) &= 2.758 \text{ eV} \\ \bar{U} - V(12^{[23]}) &= 2.562 \text{ eV} \end{aligned}$$

where $\bar{U} = \frac{U(1)+U(2)}{2}$

While these values are similar, they are quite weaker than what we found for the superconducting system. This fact may be explained by the larger distances between the cobalt and its first coordination shell. Indeed, the $3d$ magnetic orbitals have a larger volume to spread over and thus the repulsion integral is weaker.

IV. CONCLUSION

We determined the effective on-site and nearest-neighbor coupling parameters for Hubbard and $t-J$ models of the $\text{Na}_{0.5}\text{CoO}_2$ compound. The effective integrals and orbital energies were computed using ab-initio quantum chemical methods treating exactly the strong corre-

lation effects within the cobalt $3d$ shell and the screening effects up to the double-excitations.

We determined the ligand field splitting for the two crystallographically independent cobalts as well as their relative energetic ordering. As for the superconducting compound, we find the a_{1g} orbitals above the e'_g ones. The t_{2g} orbital splitting is however smaller in this system for the Co(1) atom (~ 260 meV) due to the weaker trigonal splitting. Indeed, while in the superconducting system the average distance between the oxygen and cobalt planes is 0.88\AA , in the $x = 0.5$ compound it ranges between 0.95 and 0.98\AA . As described in reference 27, the relative order between the a_{1g} and e'_g orbitals is due to a small hybridization between the t_{2g} and e_g orbitals of the regular octahedron. This hybridization is found to range between 8 and 11 degrees in this system while it was 13 degrees in the superconductor, in agreement with a larger $a_{1g}-e'_g$ splitting. The a_{1g} orbital of the Co(1) cobalt atom — on-top of a sodium cation — is found of slightly lower energy than for the Co(2) atom as expected from simple electrostatic considerations. We found that it results in a very weak charge ordering of $\pm 0.08\bar{e}$ in favor of Co(1). This weak charge ordering is in agreement BVS estimations, however in reversed order as expected from electrostatic.

As far as the hopping integrals in the t_{2g} set are concerned, none of them are zero due to the local symmetry reduction of the CoO_6 octahedra. Anyway, the dominant ones are as in the superconductor the $a_{1g}-a_{1g}$ and the $e'_{g1}-e'_{g1}$.

Finally, one should remember the strong variation of the effective exchange integrals as a function of the local distortions. This fact can of importance in the understanding of the changes in magnetic behavior of the Na_xCoO_2 compounds as a function of x . It would thus be of interest to see if the local distortions observed for larger x value will be able to reverse the sign of the magnetic exchange as supposed from neutron diffraction experiments. This point will be the object of further works.

Acknowledgments

The authors thank Daniel Maynau for providing us with the CASDI suite of programs. These calculations were done using the CNRS IDRIS computational facilities under project n°1842 and the CRIHAN computational facilities under project n°2007013.

¹ I. Terasaki, Y. Sasago and K. Uchinokura, Phys. Rev. **B 56**, R12685 (1997) ; W. Koshibae, K. Tsutsui and S. Maekawa, Phys. Rev. **B 62**, 6869 (2000).

² K. Takada, H. Sakurai, E. Takayama-Muromachi, F. Izumi, R. A. Dilanian and T. Sasali, Nature **422**, 53 (2003).

³ M. L. Foo, Y. Wang, S. Watauchi, H.W. Zandbergen, T. He, R.J. Cava and N.P. Ong, Phys. Rev. Letters **92**, 247001 (2004).

⁴ S. P. Bayracki, I. Mirebeau, P. Bourges, Y. Sidis, M. Enderle, J. Mesot, D. P. Chen, C. T. Lin, B. Keimer,

- Phys. Rev. Lett. **94**, 157205 (2005) ; L. M. Helme, A. T. Boothroyd, R. Coldea, D. Prabhakaran, D. A. Tennant, A. Hiess, and J. Kulda, Phys. Rev. Lett. **94**, 157206 (2005).
- ⁵ J. Hwang, J. Yang, T. Timusk and F. C. Chou, Phys. Rev. **B 72**, 024549 (2005).
 - ⁶ A. J. Williams, P. J. Attfield, M. L. Foo, L. Viciu and R. J. Cava, Phys. Rev. **B73**, 134401 (2006).
 - ⁷ D. N. Argyriou, O. Prokhnenko, K. Kiefer and C. J. Milne, Phys. Rev. **B 76**, 134506 (2007).
 - ⁸ P. Mendels, D. Bono, J. Bobroff, G. Collin, D. Colson, N. Blanchard, H. Alloul, I. Mukhamedshin, F. bert, A. Amato and A. D. Hillier, Phys. Rev. Lett. **14**, 136403 (2005).
 - ⁹ J. Bobroff, G. Lang, H. Alloul, N. Blanchard and G. Collin, Phys. Rev. Lett. **96**, 107201 (2006).
 - ¹⁰ N. L. Wang, Dong Wu, G. Li, X. H. Chen, C. H. Wang and X. G. Luo, Phys. Rev Lett. **93**, 147403 (2004).
 - ¹¹ K. W. Lee, J. Kuneš and W. E. Pickett, Phys. Rev. **B 70**, 045104 (2004).
 - ¹² J. Miralles, J. P. Daudey and R. Caballol, Chem. Phys. Lett. **198**, 555 (1992) ; V. M. García *et al.*, Chem. Phys. Lett. **238**, 222 (1995) ; V. M. García, M. Reguero and R. Caballol, Theor. Chem. Acc. **98**, 50 (1997).
 - ¹³ D. Muñoz, F. Illas and I. de P.R. Moreira, Phys. Rev. Letters **84**, 1579 (2000) ; D. Muñoz, I. de P.R. Moreira and F. Illas, Phys. Rev. **B 65**, 224521 (2002).
 - ¹⁴ N. Suaud and M.-B. Lepage, Phys. Rev. **B 62** 402 (2000) ; N. Suaud and M.-B. Lepage, Phys. Rev. Letters **88**, 056405 (2002).
 - ¹⁵ I. de P.R. Moreira, F. Illas, C. Calzado, J.F. Sanz J.-P. Malrieu, N. Ben Amor and D. Maynau, Phys. Rev. **B59**, R6593 (1999).
 - ¹⁶ A. Gellé and M.B. Lepage, Phys. Rev. Letters **92**, 236402 (2004) ; A. Gellé and M.B. Lepage, Eur. Phys. J. **B 43**, 29 (2005) ; Alain and M.B. Lepage, Eur. Phys. J. **B 46**, 489 (2005).
 - ¹⁷ A. Gellé and M.B. Lepage, to be published, arXiv:0711.2888.
 - ¹⁸ N. W. Winter, R. M. Pitzer and D. K. Temple, *J. Chem. Phys.* **86**, 3549 (1987).
 - ¹⁹ G. Karlström, R. Lindh, P.-Å. Malmqvist, B. O. Roos, U. Ryde, V. Veryazov, P.-O. Widmark, M. Cossi, B. Schimmelpfennig, P. Neogrady, L. Seijo, Computational Material Science **28**, 222 (2003).
 - ²⁰ D. Maynau *et al.*, CASDI suite of programs kindly provided by D. Maynau.
 - ²¹ Z. Barandiaran and L. Seijo, Can. J. Chem. **70**, 409 (1992).
 - ²² W. Koshibae and S. Maekawa, Phys. Rev. Letters **91**, 257003 (2003).
 - ²³ M. D. Johannes, I. I. Mazin, D. J. Singh and D. A. Papaconstantopoulos, Phys. Rev. Letters **93**, 9 (2004).
 - ²⁴ L.-J. Zou, J.-L. wang and Z. Zeng, Phys. Rev. **B 69**, 132505 (2004).
 - ²⁵ S. Landron and MB Lepage, Phys. Rev **B 74** 184507 (2006).
 - ²⁶ H.-B. Yang, Z.-H. Pan A. K. P. Sekharan, T. sato, S. Souma, T. Takahashi, R. Jin, B. C. Sales, D. Mandrus, A. D. Ferorov, Z. Wang and H. Ding, Phys. Rev. Lett. **95**, 146401 (2005).
 - ²⁷ S. Landron and MB Lepage, to be published in Phys. Rev. **B** (2008).
 - ²⁸ C.A. Marianetti, K. Haule and O. Parcolet, Phys. Rev. Lett. **99**, 246404 (2007).
 - ²⁹ K.-W. Lee, J. Kuneš, P. Novak and W. E. Pickett, Phys. Rev. Lett. **94**, 026403 (2005).
 - ³⁰ G. Gašparović, R. A. Ott, J.-H. Cho, F. C. Chou, Y. Chu, J.W. Lynn and Y. S. Lee, Phys. Rev. Lett **96**, 046403 (2006).